STEM CELLS®

TISSUE-SPECIFIC STEM CELLS

Comparison of Proliferative and Multilineage Differentiation Potential of Human Mesenchymal Stem Cells Derived from Umbilical Cord and Bone Marrow

DOLORES BAKSH, RAPHAEL YAO, ROCKY S. TUAN

Cartilage Biology and Orthopaedics Branch, National Institute of Arthritis, Musculoskeletal and Skin Diseases, National Institutes of Health, Department of Health and Human Services, Bethesda, Maryland, USA

Key Words. Perivascular cells • Bone marrow stromal cells • Multidifferentiation

ABSTRACT

Human umbilical cord perivascular cells (HUCPVCs) have been shown to have a high proliferative potential and the capacity to differentiate into an osteogenic phenotype. HUCPVCs have thus been considered a possible extra-embryonic mesenchymal stem cell (MSC) source for cell-based therapies. To assess this potential, we compared HUCPVCs to the "gold standard" bone marrow mesenchymal stromal cells (BMSCs) with respect to their proliferation, differentiation, and transfection capacities. HUCPVCs showed a higher proliferative potential than BMSCs and were capable of osteogenic, chondrogenic, and adipogenic differentiation. Interestingly, osteogenic differentiation of HUCPVCs proceeded more rapidly than BMSCs. Additionally, HUCPVCs expressed higher levels of CD146, a putative MSC marker, relative to BMSCs. HUCPVCs showed comparable transfection efficiency as BMSCs using a nucleofection method but were more amenable to transfection with liposomal methods (FuGENE). Gene array analysis showed that HUCPVCs also expressed Wnt signaling pathway genes that have been implicated in the regulation of MSCs. The similar characteristics between HUCPVCs and MSCs support the applicability of HUCPVCs for cell-based therapies. STEM CELLS *2007;25: 1384–1392*

Disclosure of potential conflicts of interest is found at the end of this article.

INTRODUCTION

Bone marrow represents the most commonly used tissue source of adult mesenchymal stem cells (MSCs). Bone marrow mesenchymal stromal cells (BMSCs) have been applied for cell-based therapies, including bone repair [1, 2]. However, due to the limited number of BMSCs available for autogenous use and the possibility of donor site morbidity, there is a need to identify alternative MSC sources. A recently reported potential alternative tissue source of MSCs is the connective tissue (Wharton's Jelly) of human umbilical cord (UC) [3–5]. Different harvesting procedures have led to UC-derived cells that exhibit a neuronal phenotype [3, 6] and have potential utility in treatment of neurodegenerative diseases [7, 8] or express cardiomyocyte markers [5], indicating the versatility of this cell source. However, what remains to be demonstrated is the characteristics of cells derived from Wharton's Jelly relative to the "gold standard" cell source for MSC-based therapies—BMSCs.

Sarugaser et al. postulated that the MSC population of the Wharton's Jelly matrix is located close to the vasculature of the cord and specifically isolated these cells, which they called human umbilical cord perivascular cells (HUCPVCs) [4]. Their work provided an initial characterization of HUCPVCs with respect to their nonhematopoietic phenotypic profile and capacity to generate colonies of fibroblastic and osteogenic cells. HUCPVCs were found to have a colony forming unit-fibroblast (CFU-F) frequency of about 1:300 and a population doubling time of 20 hours by passage 2, resulting in significant cell expansion and producing over 10^{10} HUCPVCs from 2–5 $\times$ 10^6 cells after 30 days of culture. Interestingly, these cells, which are major histocompatibility complex (MHC) class II negative, not only express both an immunoprivileged and immunomodulatory phenotype [9], but their MHC class I expression levels can also be manipulated [4], making them a potential cell source for MSC-based therapies. In addition, HUCPVCs represent a noncontroversial source of primitive mesenchymal progenitor cells that can be harvested after birth, cryogenically stored, thawed, and expanded for therapeutic uses.

The present work focused on directly comparing the proliferative and multilineage differentiation capacity of HUCPVCs to that of adult human BMSCs. Flow cytometry showed a higher expression of CD146, a marker expressed on both BMSCs and dental pulp MSCs [10], on HUCPVCs relative to BMSCs. Immunoselection for CD146 showed that $CD146^+$ HUCPVCs had the capacity to differentiate down the osteogenic, adipogenic, and chondrogenic lineages. In addition, using standard transfection protocols, HUCPVCs were found to be amenable to gene transfection. Finally, we used gene array analysis to demonstrate the expression of components of Wnt signaling pathways, which are important in the regulation of adult MSC activities in HUCPVCs. These findings further support the potential utility of HUCPVCs for cell-based therapeutic applications.

Correspondence: Rocky S. Tuan, Ph.D., Cartilage Biology and Orthopaedics Branch, National Institute of Arthritis and Musculoskeletal and Skin Diseases, 50 South Dr., Room 1503, BMSC 8022, National Institutes of Health, Bethesda, Maryland 20892-8022, USA. Telephone: 301-451-6854; Fax: 301-435-8017; e-mail: tuanr@mail.nih.gov Received November 13, 2006; accepted for publication February 13, 2007; first published online in STEM CELLS *EXPRESS* March 1, 2007. 1066-5099/2007/$30.00/0 doi: 10.1634/stemcells.2006-0709

MATERIALS AND METHODS

Isolation and Culture of HUCPVCs and BMSCs

HUCPVCs were isolated from umbilical cords ($n = 3$) from consenting patients who underwent full-term caesarian sections according to the methods described by Sarugaser et al. [4] and were generously provided by Dr. J.E. Davies (University of Toronto, Canada). BMSCs were harvested according to the Institutional Review Board protocol (George Washington University and National Institutes of Health) from the hips of consenting patients ($n = 3$). For both cell types, adherent cells were maintained in monolayer culture in Dulbecco's modified Eagle's medium (DMEM) (Gibco, Grand Island, NY, http://www.invitrogen.com) supplemented with 10% fetal bovine serum (FBS) from selected lots (HyClone, Logan, UT, http://www.hyclone.com). Passage 3 cells were used for subsequent studies.

Phenotypic Analysis

Standard flow cytometry techniques were used to determine the cell surface epitope profile (CD49e, CD90, CD146, CD31, CD117, CD45, CD34, and Stro-1) of HUCPVCs and BMSCs. Briefly, HUCPVCs and BMSCs were incubated with saturating concentrations (1:70) of conjugated mouse monoclonal antibodies to human CD49e-phycoerythrin (PE), CD90-allophycocyanin (APC), CD146-PE, CD31, CD117-PE, CD34-PE, and CD45-PE (all antibodies were purchased from BD Biosciences, San Diego, http://www.bdbiosciences.com). Cells were incubated for 1 hour at 4°C. Stro-1 antibody detection involved incubating the cells in 200 μl of saturating concentrations of mouse IgM monoclonal antibody Stro-1 (American Type Culture Collection, Manassas, VA, http://www.atcc.org) for 30 minutes at 4°C. Prior to antibody labeling, the cells were preincubated with 1% human, goat, and mouse sera for 10 minutes. Subsequently, to block nonspecific binding, the cells were washed twice with phosphate-buffered saline (PBS) containing 2% FBS and then incubated with PE-conjugated rat anti-mouse IgM monoclonal secondary antibody (BD Biosciences). All cell suspensions were washed twice with PBS and resuspended in PBS + 2% FBS for analysis on a flow cytometer (FACSCalibur; BD Biosciences) using the CellQuest software. Positive staining was defined as the fluorescence emission that exceeded levels obtained by more than 99% of cells from the population stained with the corresponding negative controls. The isotype (negative) controls used in these studies were IgG_1-PE and IgG_1-APC (BD Biosciences).

Cell Proliferation Assays

HUCPVCs and BMSCs were plated at 3×10^3 cells per cm^2 in 12-well plates in basal medium (10% FBS in DMEM). Medium was refreshed every 3 days. On days 3, 7, 14, and 20, 3-(4,5-dimethylthiazol-2-yl)-5-(3-carboxymethoxyphenyl)-2-(4-sulfophenyl)-2H-tetrazolium assay was performed according to manufacturer's protocol (Promega, Madison, WI, http://www.promega.com).

Multilineage Differentiation Assays

Osteogenesis. Cells were grown in osteogenic growth medium (10 nM dexamethasone [DEX], 5 mM β-glycerophosphate, 50 μg/ml ascorbic acid [AA], and 10 nM 1,25-dihydroxy vitamin D_3) (all reagents purchased from Sigma-Aldrich, St. Louis, http://www.sigmaaldrich.com). On day 21, cultures were stained for alkaline phosphatase (ALP; Sigma) activity and mineralization was assessed by von Kossa staining (2% silver nitrate; Sigma) after 5 weeks. Quantification of ALP activity was determined by adding 4 mg/ml *p*-nitrophenyl phosphate (Sigma) in an alkaline buffer solution (221 Alkaline Buffer Solution; Sigma) into each well, followed by incubation for 15 minutes at 37°C. The reaction was terminated with 0.05 N NaOH, and ALP activity was estimated spectrophotometrically on the basis of A_{405}, determined using a microplate reader.

Chondrogenesis. Cells were grown as high-density pellets (2.5×10^5 cells) for 21 days in serum-free medium (DMEM, ITS Premix [BD Biosciences], 50 μg/ml AA, 40 μg/ml L-proline, 100 μg/ml sodium pyruvate, 0.1 μM DEX) with and without 10 ng/ml recombinant human transforming growth factor (TGF)-β3 (R&D Systems Inc., Minneapolis, http://www.rndsystems.com). On day 21, pellets were prepared for histology to detect sulfated glycosaminoglycan (sGAG) (Alcian Blue staining) and collagen content (picrosirius red staining). sGAG content was quantified using the Blyscan sGAG assay (Accurate Chemical & Scientific Corp., Wesbury, NY, http://www.accuratechemical.com).

Adipogenesis. Cells were cultured as a monolayer in the presence of adipogenic supplements (1 μM DEX, 1 μg/ml insulin, and 0.5 mM 3-isobutyl-1-methylxanthine; Sigma). On day 21, cultures were stained with oil red O stain (Sigma), and dye content was quantified by isopropanol elution and spectrophotometry.

Histology of Human Umbilical Cord

Human umbilical cord cryosections were generously prepared and provided by Jane Ennis (University of Toronto, Canada). Sections were stained with Harris hematoxylin (Sigma) and counterstained in aqueous eosin (Sigma) (H&E). Sections were also stained with CD146-PE or with an isotype control (IgG_1-PE; BD Biosciences) following the methods described above and counterstained with Hoechst nuclear dye. Immunostained sections were observed with epifluorescence optics (Leitz, Heerbrugg, Switzerland).

Fluorescence-Activated Cell Sorting

HUCPVCs were incubated with saturating concentrations (1:100 dilution) of conjugated mouse $IgG_{1,\kappa}$ anti-human CD146e-PE (BD Biosciences). Both the CD146-negative and CD146-positive cells were sorted on a MoFlo Cell Sorter (Dako, Glostrup, Denmark, http://www.dako.com) at a rate of 2,000–3,000 cells per second at 10.5 psi to 98% purity. The sorted populations were cultured under osteogenic, adipogenic, and chondrogenic conditions.

Transfection Efficiency

To assess the efficiency of commonly used transfection protocols, HUCPVCs were transfected with DsRed (Clontech, Palo Alto, CA, http://www.clontech.com) by means of FuGENE 6 Transfection Reagent (Roche Diagnostics, Basel, Switzerland, http://www.roche applied-science.com), Effectene Transfection Reagent (Qiagen, Hilden, Germany, http://www.qiagen.com), and nucleofection (amaxa biosystems, Gaithersburg, MD, http://www.amaxa.com). The total mass of DNA to volume of FuGENE reagent used was 2:3 in the FuGENE protocol. Effectene transfection was performed according to the manufacturer's protocol for adherent cells. Nucleofection with amaxa reagent was according to the methods described by Haleem-Smith et al. [11]. Briefly, 5×10^5 cells were incubated with 2 μg of DsRed cDNA and resuspended in 100 μl of nucleofection reagent and subject to electroporation using the manufacturer's protocol (amaxa). After 4 days post-transfection, the expression of DsRed was assessed by fluorescence microscopy and quantified by flow cytometry. To monitor the long-term stability of exogenous gene expression, positive DsRed expression was determined using flow cytometry on days 4, 7, 14, and 21 post-transfection. As control, BMSCs were similarly transfected.

Wnt Signaling Pathway

Expression of Wnt Signaling Components. To compare the Wnt signaling pathway molecular profile between HUCPVCs and BMSCs, RNA was harvested from both HUCPVCs and BMSCs (passage 3, $n = 2$) and analyzed, following manufacturer's recommended protocol, on an Oligo GEArray Human Wnt Signaling Pathway Microarray (catalogue number: OHS-043; SuperArray Bioscience Corporation, Frederick, MD, http://www.superarray.com).

Canonical Wnt Responsive Reporter Assay. An optimized version of the TOP-FLASH luciferase reporter plasmid (pLG3-OT) (kindly provided by Dr. Bert Vogelstein, Johns Hopkins University) was used to assay canonical Wnt-responsive transcriptional activity in HUCPVCs relative to BMSCs. Cells were cotransfected by nucleofection (amaxa) with expression constructs of Wnt3a and Wnt5a and empty vector (control) (all purchased from Upstate, Charlottesville, VA, http://www.upstate.com) and Renilla luciferase

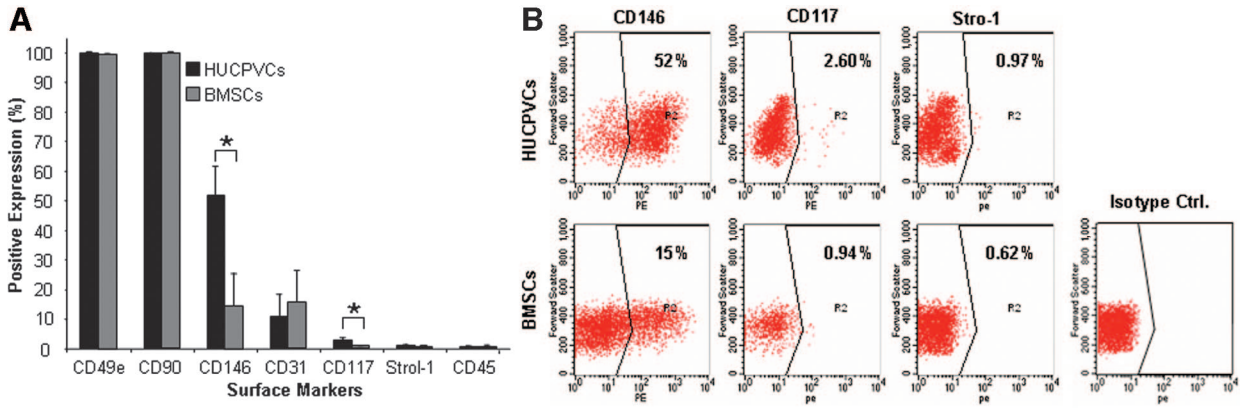

Figure 1. Profile of cell surface epitopes in HUCPVCs and BMSCs. **(A):** Abundance of cells positive for CD49e, CD90, CD146, CD31, CD117, Strol-1, and CD45, expressed as percentages, in HUCPVCs and bone marrow-derived BMSCs. Bars represent mean ± SD of $n = 3$ donor samples; *, $p < .05$. **(B):** Representative flow cytometric plots, including isotype control (IgG_1-PE). Dots in R2 represent positive expression. Flow cytometric analysis confirmed that HUCPVCs are nonhematopoietic cells; however, they express elevated levels of CD146. Abbreviations: BMSCs, bone marrow mesenchymal stromal cells; Ctrl., control; HUCPVCs, human umbilical cord perivascular cells; PE, phycoerythrin; R2, region 2.

plasmid (1 μg) under the control of the cytomegalovirus promoter (Promega) and TOP-FLASH luciferase plasmid (2 μg). Luciferase activity was assayed using the Dual Luciferase Assay System according to the manufacturer's protocol (Promega) and reporter luciferase activity normalized to that of Renilla luciferase.

Data Analysis

Data are presented as mean ± SD for at least three independent experiments (different patient samples) performed in triplicate, unless stated otherwise. Statistical significance is determined by analysis of variance and set at $p < .05$.

RESULTS

Phenotypic Profile of HUCPVCs

Flow cytometric analyses of passage 3 cells revealed that HUCPVCs represent a nonhematopoietic cell population ($CD45^-$ expression) comparable to BMSCs (Fig. 1A). However, HUCPVCs expressed statistically higher levels of CD146 and CD117 compared with BMSCs (Fig. 1A, 1B). Dual-labeling of CD146 with CD31, CD34, or CD45 showed that HUCPVCs had a $CD45^-/CD34^-/CD31^-/CD146^+$ phenotype (data not shown).

Proliferative Potential

MTS assay of passage 3 HUCPVCs and BMSCs showed similar proliferation profiles (data not shown). However, between days 7 and 14, HUCPVCs increased their rate of growth relative to BMSCs, which corresponded to a significant increase in cumulative population doublings and a reduction in population doubling time (Fig. 2A, 2B). By day 20, HUCPVCs and BMSCs had undergone 2.8 ± 0.35 and 1.82 ± 0.12 population doublings, respectively. However, beyond day 20, BMSCs experienced contact-inhibited growth and no longer proliferated, whereas HUCPVCs continued to grow by multilayering (results not shown). Throughout the assay period, both cells types maintained similar cell morphology (i.e., elongated and spindled-shaped) (day 7 results shown) (Fig. 2C).

Multilineage Differentiation Potential

The differentiation potential of HUCPVCs and BMSCs was tested by culturing under multidifferentiation conditions. Under osteogenic conditions, HUCPVCs expressed higher ALP activity by day 21 relative to BMSCs (Fig. 3Ai–3Aiv). Furthermore, von Kossa staining at 5 weeks revealed a greater extent of mineralization with more detectable bone nodules in osteogenic cultures of HUCPVCs than in those of BMSCs (Fig. 3Av–3Aviii, 3B). Mineralization was detected earlier in HUCPVCs than in BMSCs cultured under osteogenic conditions (day 10 vs. day 14, respectively).

High density cell pellets of HUCPVCs cultured under chondrogenic conditions (+TGF-β3) produced slightly larger pellets as compared to those generated from BMSCs by day 21 (data not shown). When chondrogenic pellets were examined histologically, the staining intensities of Alcian Blue (Fig. 4Ai, 4Aiii) and picrosirius (Fig. 4Aii, 4Aiv) were comparable between HUCPVCs and BMSCs. Biochemical analysis also showed comparable sGAG levels at later time points (Fig. 4B); however, a significant difference in sGAG content between HUCPVCs and MSCs was seen only on day 7.

Interestingly, oil red O staining showed that HUCPVCs generated significantly more fat-containing cells than BMSCs when grown under adipogenic conditions by day 21 (Fig. 4Ci–4Civ). Fat-containing cells were first detected by day 12 of culture for both HUCPVCs and BMSCs. Quantitation of dye content in the adipogenic cultures confirmed the histochemical observations (Fig. 4D).

Expression of CD146 in Human Umbilical Cord

H&E staining of human UC revealed areas containing high and low cell densities (Fig. 5A), which correlated with nuclear dye staining (Fig. 5B). Specifically, H&E staining showed a clear demarcation of the vessel lumen, vessel wall (VW), and perivascular region (PVR) (Fig. 5A). Incubation with CD146 and nuclear staining showed that CD146 was highly prevalent in the PVR region with diffuse staining in the VW region (Fig. 5C). $CD146^+$ cells were not readily detected in the bulk Wharton's Jelly region from these cord samples.

$CD146^+$ HUCPVCs Are Capable of Multilineage Differentiation Potential

Both immunostaining for CD146 of human UC and flow cytometric analysis of HUCPVCs revealed that a large fraction of cells expressed CD146 (Fig. 1). To assess the functional significance of the expression of CD146, HUCPVCs were sorted into $CD146^+$ and $CD146^-$ cell populations that were then cultured under differentiation conditions. Under adipogenic (Fig. 5E, 5F, 5I), osteogenic (Fig. 5G, 5H, 5K), and chondrogenic (Fig. 5K–5N) conditions, $CD146^+$ sorted HUCPVCs showed the

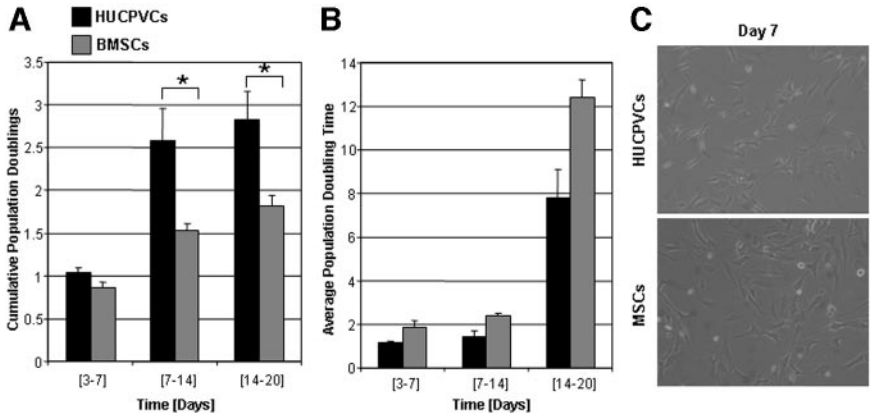

Figure 2. Proliferative potential of HUCPVCs and BMSCs. **(A):** Cumulative population doublings and **(B)** average population doubling time. We used 3-(4,5-dimethylthiazol-2-yl)-5-(3-carboxymethoxyphenyl)-2-(4-sulfophenyl)-2H-tetrazolium assay to determine total cell number in HUCPVC and BMSC cultures at days 3, 7, 14, and 20 after plating and, from these values, the cumulative population doublings and average population doubling time were calculated. After 14 days, HUCPVCs exhibited a greater proliferative potential relative to BMSCs. Bar represents mean ± SD, $n = 3$, triplicate; ∗, $p < .05$. **(C):** Morphology. Representative phase-contrast images of HUCPVCs and BMSCs on day 7. In both cultures, cells appeared elongated and spindled-shaped. Abbreviations: BMSCs, bone marrow mesenchymal stromal cells; HUCPVCs, human umbilical cord perivascular cells.

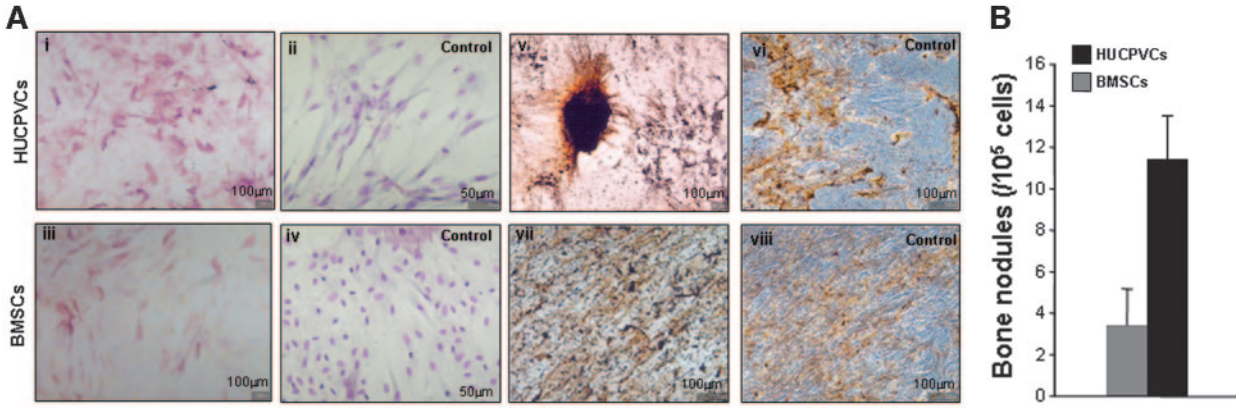

Figure 3. Osteogenic potential of HUCPVCs and BMSCs. **(A):** Osteogenesis. (i–iv): Alkaline phosphatase (ALP) staining. Representative images of day-21 osteogenic cultures (i, iii) stained for ALP. Control cultures (ii, iv, nonosteogenic conditions) were stained in parallel. (v–viii): Mineralization. von Kossa-stained osteogenic cultures after 5 weeks. Bone nodules were typically observed in HUCPVCs cultured under osteogenic conditions by week 3, whereas by week 5 of osteogenic culture, bone nodules were detected in BMSC cultures. **(B):** Quantification of bone nodules. Bone nodules staining positive for von Kossa were counted from HUPCVC and BMSC cultures at 5 weeks. Abbreviations: BMSCs, bone marrow mesenchymal stromal cells; HUCPVCs, human umbilical cord perivascular cells.

capacity to differentiate into the corresponding differentiated phenotypes. No significant adipogenic, osteogenic, and chondrogenic capacity was detected from the $CD146^-$ sorted HUCPVC population (data not shown).

Transfection Efficiency

To assess transfection capacity, HUCPVCs and BMSCs were transfected with a DsRed plasmid construct using an electroporation-based method (amaxa) and two different types of standard liposomal transfection methods (FuGENE and Effectene). After 4 days post-transfection, fluorescence microscopy showed similar levels of DsRed positive cells from HUCPVCs and BMSCs transfected by nucleofection (Fig. 6A, 6B), whereas slightly different numbers of DsRed positive cells were seen from FuGENE and Effectene transfected HUCPVCs and BMSCs (Fig. 6C–6F). Flow cytometry quantified the relative difference in transfection efficiency between the different methods for both HUCPVCs and BMSCs (Fig. 6G). In general, nucleofection resulted in ~50% cell death but high transfection efficiency, whereas transfection with FuGENE and Effectene resulted in ~90% cell viability but lower transfection efficiency. Interestingly, HUCPVCs demonstrated higher transfection efficiencies with FuGENE and Effectene compared with BMSCs (Fig. 6G).

Stability of expression of the transfected gene was next examined by flow cytometry analysis of DsRed cells at days 4, 7, 14, and 21 post-transfection. For all methods used, HUCPVCs had the greatest expression of DsRed by day 4 but lost a significant amount of DsRed expression after 14 days post-transfection (Fig. 6H). Interestingly, even in the nucleofection group, which represented the highest transfection efficiency relative to the other groups, HUCPVCs lost >80% of DsRed expression from day 4 to day 21, whereas BMSCs lost only 45% expression of DsRed from day 4 to day 21 (Fig. 6H).

Wnt Signaling Pathway Profile of HUCPVCs

As a first screen to assess biological and functional similarities between HUCPVCs and BMSCs at the molecular level, HUCPVCs and BMSCs were compared using a Wnt pathway focused oligo gene array (SuperArray Biosciences) designed to profile the expression of genes involved in and downstream of Wnt signaling. The Wnt signaling pathway is represented on the

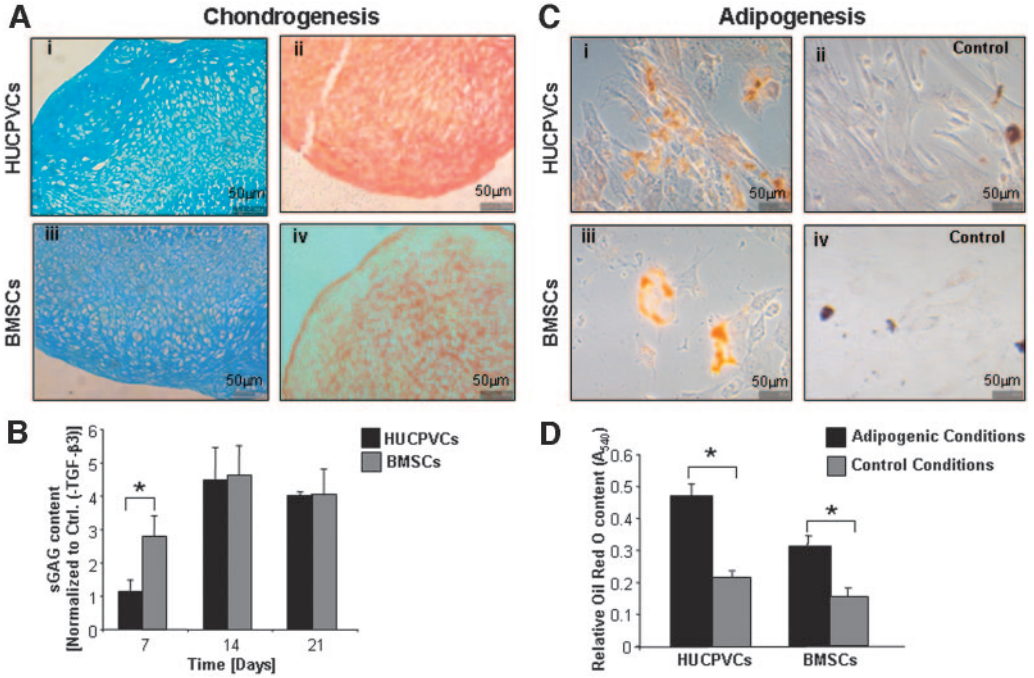

Figure 4. Chondrogenic and adipogenic potential of HUCPVCs and BMSCs. **(A):** Chondrogenesis—histology. Representative pellets stained for sGAG with Alcian Blue staining (i, iii) and for collagen with picrosirius red staining (ii, iv). **(B):** Chondrogenesis—sGAG content on days 7, 14, and 21. HUCPVCs displayed similar levels of Alcian Blue staining and sGAG production but exhibited more intense collagen staining compared with BMSCs. **(C):** Adipogenesis—histology. Representative images of oil red O stained HUCPVCs (i) and BMSCs (iii) grown under adipogenic conditions. Control cultures (basal medium) were stained in parallel (ii, iv). Significantly, more lipid-positive cells were seen in HUCPVC cultures than BMSC cultures grown in adipogenic conditions. **(D):** Adipogenesis—quantification of oil red O. Higher level of staining was seen in HUCPVCs. Each bar represents the mean ± SD ($n = 3$, triplicate); ∗, $p < .05$. Abbreviations: BMSCs, bone marrow mesenchymal stromal cells; Ctrl., control; HUCPVCs, human umbilical cord perivascular cells; sGAG, sulfated glycosaminoglycan; TGF, transforming growth factor.

array by genes encoding the 19 glycosylated extracellular signaling molecules of the Wnt family, cell-surface receptors serving as ligands of Wnt genes (e.g., Frizzled receptors), intracellular signaling molecules and target genes involved in the cell cycle, and growth regulation and proliferation, regulators of the Wnt signaling pathway and competitive Wnt binding antagonists, and genes involved in protein modification, as a result of kinase and phosphatase activity and ubiquitination, downstream of Wnt signaling. Analysis of the gene arrays (Fig. 7A, 7B) was performed using the manufacturer's computer software to determine differential gene expression of Wnts and Frizzled in HUCPVCs and BMSCs (Fig. 7C, 7D). The results revealed that HUCPVCs expressed lower levels of Wnt1, Wnt5a, and Wnt5B (Fig. 7C) and lower levels of Fz1, Fz5, and Fz7 but a higher level of Fz2 (Fig. 7D), relative to BMSCs. There were no significant differences between HUCPVCs and BMSCs in the gene expression of all the other Wnts and Frizzled receptors (data not shown). We also observed that DKK1 and PITX2 were overexpressed (Fig. 7E), whereas a number of downstream Wnt signaling molecules were underexpressed, in HUCPVCs relative to BMSCs (Fig. 7F).

Canonical Wnt Signal Transduction

To assess the functional status of canonical Wnt signaling, HUCPVCs and BMSCs were cotransfected by nucleofection with the TOP-FLASH reporter construct and with either expression constructs of Wnt3a (a canonical Wnt) or Wnt5a (a noncanonical Wnt) or empty vector (control). The TOP-FLASH reporter luciferase activity measures the β-catenin-LEF/TCF transcriptional activity, the target of canonical Wnt signaling pathway. Similar levels of β-catenin-LEF/TCF transcriptional activities were seen in HUCPVCs and BMSCs under all conditions studied (Fig. 7F). Of particular importance, cotransfection of Wnt3a significantly enhanced reporter activity in both HUCPVCs and BMSCs relative to empty vector control conditions, whereas transfection with Wnt5a significantly reduced reporter activity relative to Wnt3a transfected conditions. This finding indicates the canonical specificity of the Wnt signaling response seen in these cells.

DISCUSSION

The direct comparison reported here showed that HUCPVCs and BMSCs share common cell surface epitopes and the ability to undergo multilineage mesenchymal differentiation. HUCPVCs exhibit a higher rate of proliferation and osteogenic differentiation and are also amenable to gene transfection using nonviral approaches and express functional Wnt signaling capability.

The nonhematopoietic nature of HUCPVCs is suggested by their lack of cell surface expression of CD45 [3, 4]. Our analysis of a variety of cell surface markers on HUCPVCs relative to BMSCs confirmed the nonhematopoietic phenotype of HUCPVCs and revealed a similar epitope profile to BMSCs, including Stro-1, a well accepted MSC marker [12] (Fig. 1A). However, the expression of CD146 was most notably elevated in HUCPVCs relative to BMSCs, both as a harvested cell population from the perivascular region as well as by direct immunostaining of umbilical cord (Fig. 5C). CD146 is characteristically expressed on circulating endothelial cells, which also express CD31, a classic endothelial marker [13]. However, the expression of CD146 on circulating endothelial cells is rarely found in the blood circulation of healthy individuals, but rather

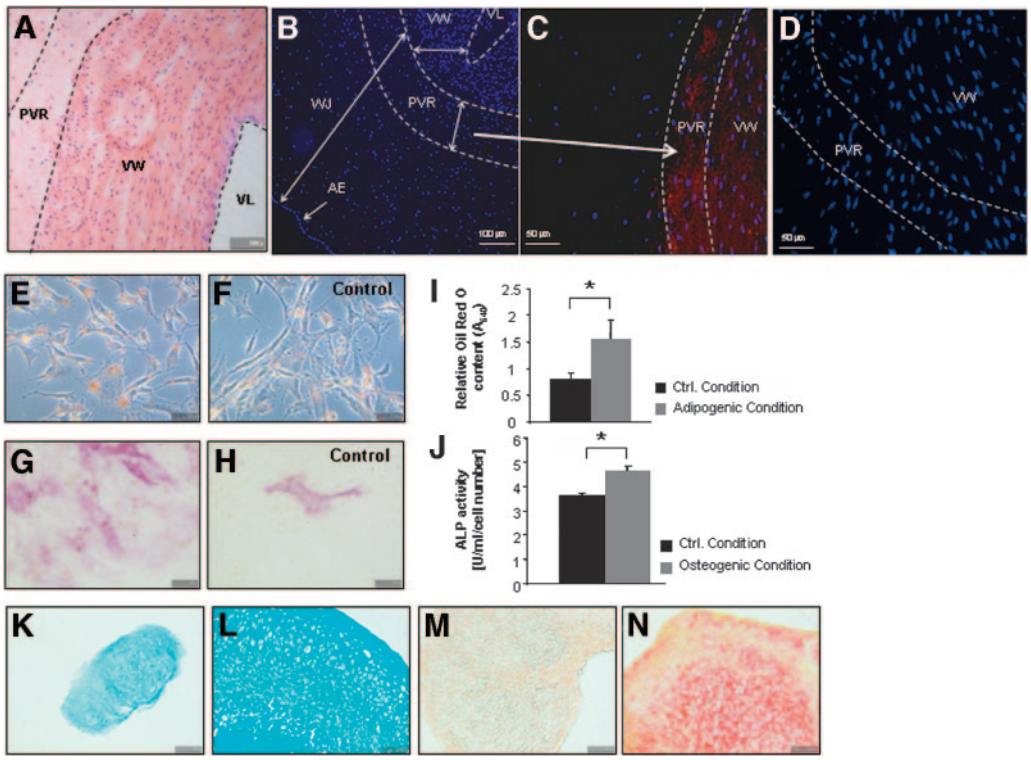

Figure 5. Immunolocalization of CD146 in human umbilical cord and multilineage potential of CD146$^+$-sorted HUCPVCs. **(A–D):** Immunofluorescence. **(A):** H&E staining of cryosections of human umbilical cord (UC) revealing the perivascular region, vessel wall, and vessel lumen. **(B):** Hoechst nuclear dye staining of human UC revealing the cell density distribution from the VL, VW, PVR, bulk Wharton's Jelly region to the AE. **(C):** Higher magnification image of human UC section stained with CD146-phycoerythrin. **(D):** Negative control (isotype control) image of human UC section costained with Hoechst nuclear dye. Fluorescence imaging revealed a high incidence of CD146-positive cells in the PVR. **(E–N):** Multilineage differentiation. Human umbilical cord perivascular cells (HUCPVCs) were sorted on the basis of CD146 expression and were subsequently cultured under adipogenic, osteogenic, and chondrogenic conditions. **(E, F):** Representative oil red O stained cultures after 21 days of HUCPVCs grown in adipogenic **(E)** and control **(F)** medium. **(G, H):** Representative ALP-stained HUCPVC cultures after 21 days in osteogenic **(G)** and control medium **(H)**. **(I):** Quantitation of oil red O staining in adipogenic cultures. **(J):** Quantitation of ALP activity in osteogenic cultures. Each bar represents the mean ± SD, $n = 3$, triplicate; *, $p < .05$. **(K, L):** Alcian Blue-stained pellets of HUCPVCs grown for 21 days with or without 10 ng/ml transforming growth factor-β3 ([**K**] and [**L**], respectively) for chondrogenesis analysis. **(M, N):** Picrosirius red-stained pellets of similar cultures as in **(K)** and **(L)**. Results indicated that CD146$^+$-sorted HUCPVCs have the potential to differentiate along the adipogenic, osteogenic, and adipogenic lineages. Abbreviations: AE, amniotic epithelium; ALP, alkaline phosphatase; Ctrl., control; PVR, perivascular region; VL, vessel lumen; VW, vessel wall; WJ, Wharton's Jelly.

is present in a number of diseased conditions, which include inflammatory, immune, infectious, neoplastic, and cardiovascular disease [14], and has thus been considered a useful marker of cells applicable for therapeutic neovascularization and vascular repair [15]. We confirmed by coimmunostaining of CD146 with CD31 that CD146$^+$ HUCPVCs are not endothelial in origin due to the lack of CD31 expression. Our results, in part, corroborate with those of Shi et al., who demonstrated that Stro-1$^+$ BMSCs express CD146, and that this population could give rise to CFU-Fs [10]. Our work, however, extends upon these observations and shows that a CD146$^+$-sorted HUCPVC population has the capacity to differentiate down the osteogenic, chondrogenic, and adipogenic mesenchymal lineages. Taken together, these results infer a potential novel role of HUCPVCs to circulate in biological fluid, similar to CD146$^+$ endothelial cells, and participate in the repair of diseased and/or damaged tissue. In future studies, the capacity of HUCPVCs to transit biological fluid and "home" to organs of the body will be examined in appropriate animal models.

HUCPVCs demonstrated a greater proliferative capacity when compared with BMSCs, especially after 7 days of culture, as shown by a significant difference in cumulative population doublings (Fig. 2A). Interestingly, after 20 days, HUCPVCs did not experience contact-inhibited cell growth, unlike BMSCs, which failed to continue to proliferate after reaching 100% surface confluence. HUCPVCs continued to grow by cell multilayering and formed aggregates overlying a layer of confluent cells. These cell aggregates contained live cells as determined by trypan blue exclusion, and when transferred to a new tissue culture flask, these cell aggregates demonstrated the capacity to plate out and proliferate to colonize the culture substrate (data not shown). Using a Cancer Pathway Finder Gene Array (SuperArray Biosciences), we have ruled out the possible transformation to a cancer phenotype of HUCPVCs generated from these aggregates (data not shown). However, we are currently examining the changes in the cell surface membrane expression of a variety of adhesion molecules to identify the molecular mechanism involved in this phenomenon.

Our results also showed that HUCPVCs, as a population, have multilineage differentiation capacity. Importantly, HUCPVCs undergo osteogenesis at a faster rate than BMSCs, based on the increase in ALP positive cells (Fig. 3A), and after 5 weeks of culture under osteogenic conditions, HUCPVCs generated a greater extent of mineralization than BMSCs, including bone nodule generation (Fig. 3B). This difference may be attributed to the fact that the initial cell isolate of HUCPVCs has a higher frequency of osteoprogenitor cells [4] than bone marrow-derived BMSCs [16]. Nevertheless, this finding may

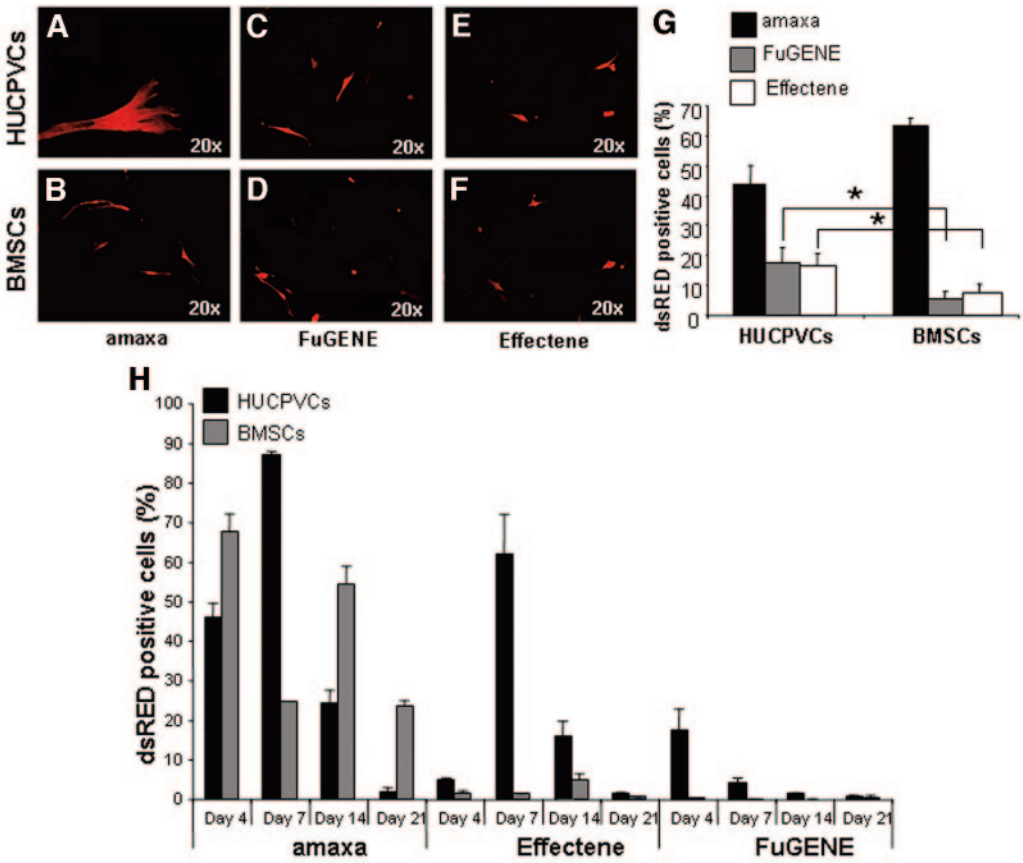

Figure 6. Transfection efficiency of HUCPVCs. **(A–F):** Representative fluorescence images revealing DsRed-positive cells after 4 days post-transfection with amaxa, FuGENE, and Effectene. **(G):** Quantitation of DsRed-positive expression (% of total cells) for each transfection method. Each bar represents the mean ± SD, $n = 3$, triplicate; *, $p < .05$. **(H):** Long-term monitoring of DsRed expression for each transfection method. HUCPVCs demonstrated a higher transfection efficiency using FuGENE and Effectene relative to BMSCs, although long-term retention of transgene activity was less efficient in nucleofection-transfected HUCPVCs. Abbreviations: BMSCs, bone marrow mesenchymal stromal cells; HUCPVCs, human umbilical cord perivascular cells.

render HUCPVCs a readily available source of cells for orthopaedic and tissue engineering strategies, which require suitable cells for abundant matrix synthesis [17]. Furthermore, cartilaginous pellets derived from HUCPVCs displayed an extracellular matrix that stained positive for sGAG and collagen, similar to that seen in cultures of BMSCs. As such, HUCPVCs may also be considered a viable cell source for adult human cartilage repair [18]. Studies are underway to evaluate the mechanical properties of the elaborated chondrogenic matrix according to the methods described by Mauck et al. [19].

Cell-based strategies may inevitably involve the introduction of transgenes into the donor cell population and, thus, in order to evaluate HUCPVCs as a candidate cell source for a variety of gene-based strategies, we studied the transfectability of HUCPVCs using conventional and established transfection methods for mammalian cells. FuGENE and Effectene transfection reagents were chosen, as they represent nontoxic methods (high cell viability) of introducing DNA into cells [20], whereas nucleofection using the amaxa system provides high transfection efficiency but lower cell viability [11]. Nucleofection resulted in the highest transfection efficiency for both HUCPVCs and BMSCs (>50% of DsRed expression) but the highest cell death, as determined by propidium iodide staining, (~50%) relative to FuGENE and Effectene (<2%) (data not shown). Interestingly, HUCPVCs were also transfectable using FuGENE (~18%), whereas BMSCs showed marginal DsRed expression with FuGENE (Fig. 6). The results observed for BMSCs with FuGENE are consistent with those reported by others [21]. The ability to introduce exogenous DNA into HUCPVCs using conventional methods, which are straightforward and allow for high-throughput, renders HUCPVCs a promising MSC candidate source of cells for gene therapy approaches, similar to BMSCs [22, 23]. However, despite the higher transfection efficiency with nucleofection, HUCPVCs lost DsRed expression at a faster rate compared with BMSCs (Fig. 5H), suggesting a possibly different mode of transgene incorporation; the higher proliferative rate observed in HUCPVCs relative to BMSCs may also interfere with long-term transgene stability. Viral methods of transgene incorporation may thus be a more effective approach to achieve long-term transgene incorporation in HUCPVCs [24]. However, for short-term studies, HUCPVCs represent a useful cell type for the introduction of transgenes using conventional methods, resulting in high cell viabilities.

To further examine the biological characteristics of HUCPVCs, we employed a gene array approach to compare the Wnt signaling pathway gene expression profiles of HUCPVCs and BMSCs. We and others have shown that the Wnt signaling pathways play a critical role in the maintenance and osteogenic potential of bone marrow-derived BMSCs [25, 26] and may be modulated to enhance bone repair in a variety of human diseases, such as osteoporosis and osteosarcoma. Our results showed that HUCPVCs ex-

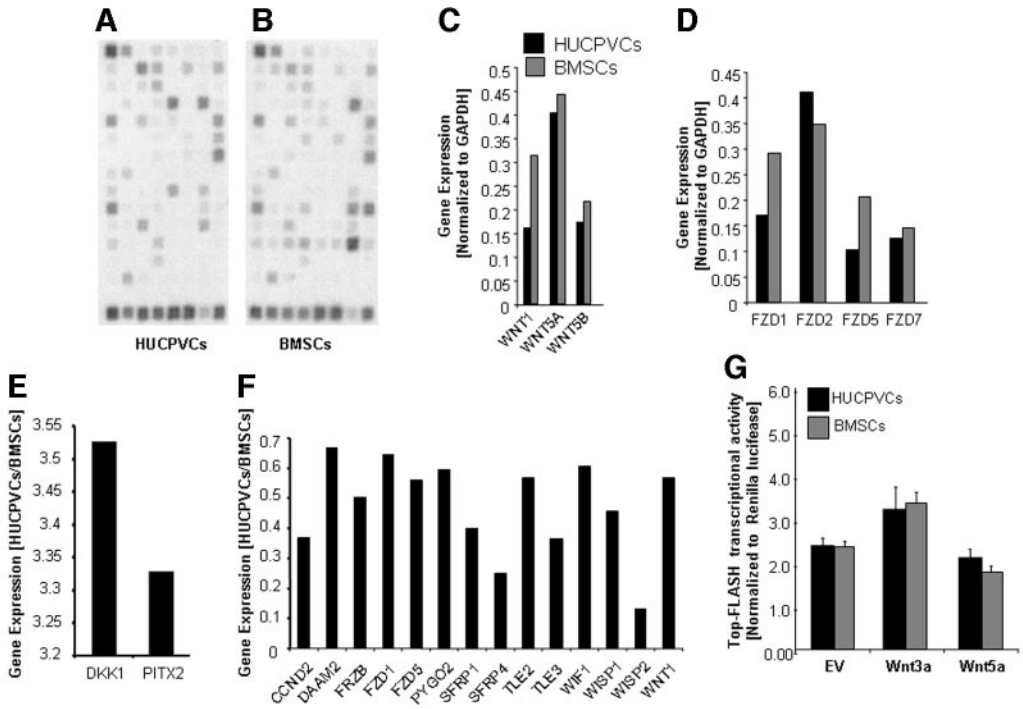

Figure 7. Wnt signaling profile of HUCPVCs. **(A–F):** Gene expression profile analyzed using Wnt signaling gene arrays. Representative gene array for **(A)** HUCPVCs and **(B)** BMSCs. **(C, D):** Comparison of Wnt and Frizzled receptor expression in HUCPVCs and BMSCs showing only those genes expressed at different levels in HUCPVCs and BMSCs. **(E, F):** Overexpressed and underexpressed genes, respectively, in HUCPVCs relative to BMSCs. Each bar represents the mean ($n = 2$). **(G):** Wnt signaling transduction potential was assessed in HUCPVCs and BMSCS by cotransfection of cells with expression constructs of Wnt3a, Wnt5a, and empty vector and the TOP-FLASH reporter. Cells were also transfected with Renilla luciferase to control for transfection efficiency. Each bar represents the mean ± SD ($n = 3$, triplicate). There were no statistical differences calculated within and between groups ($p > .05$). Results indicate that HUCPVCs possess the molecular machinery to signal through the canonical Wnt signaling pathway. Abbreviations: BMSCs, bone marrow mesenchymal stromal cells; EV, empty vector; GAPDH, glyceraldehyde-3-phosphate dehydrogenase; HUCPVCs, human umbilical cord perivascular cells.

press genes of Wnt signaling pathways, and the profile was generally similar to that of BMSCs except for several over- and underexpressed genes, such as DKK1/Fz2 and Wnt1/Fz1, respectively (Fig. 7). The functional significance of these differences is currently being studied. Importantly, HUCPVCs demonstrated the capacity to transduce canonical Wnt signaling in response to Wnt3a, a canonical Wnt, which was blocked when Wnt5a, a noncanonical Wnt, was transfected into the cells (Fig. 7G). Taken together, these findings reveal that HUCPVCs and BMSCs share common Wnt signaling pathways and, thus, the tools and reagents used to study Wnt signaling pathways in other cell systems, including BMSCs, can be applied to HUCPVCs.

In summary, our work demonstrates that HUCPVCs represent a nonhematopoietic, nonendothelial cell population with the capacity to proliferate and differentiate down the osteogenic, chondrogenic, and adipogenic lineages. The results from our direct comparison of HUCPVCs to BMSCs further support HUCPVCs as a candidate MSC population for cell-based therapeutic strategies.

ACKNOWLEDGMENTS

The authors thank Jane Ennis, Ph.D. graduate student, University of Toronto, Canada, for providing the human umbilical cord cryosections used in these studies. This work is supported by the Intramural Research Program of NIAMS, NIH (Z01AR41131).

DISCLOSURE OF POTENTIAL CONFLICTS OF INTEREST

The authors indicate no potential conflicts of interest.

REFERENCES

1 Arinzeh TL, Peter SJ, Archambault MP et al. Allogeneic mesenchymal stem cells regenerate bone in a critical-sized canine segmental defect. J Bone Joint Surg Am 2003;85-A:1927–1935.
2 Bruder SP, Kurth AA, Shea M et al. Bone regeneration by implantation of purified, culture-expanded human mesenchymal stem cells. J Orthop Res 1998;16:155–162.
3 Mitchell KE, Weiss ML, Mitchell BM et al. Matrix cells from Wharton's jelly form neurons and glia. STEM CELLS 2003;21:50–60.
4 Sarugaser R, Lickorish D, Baksh D et al. Human umbilical cord perivascular (HUCPV) cells: A source of mesenchymal progenitors. STEM CELLS 2005;23:220–229.
5 Wang HS, Hung SC, Peng ST et al. Mesenchymal stem cells in the Wharton's jelly of the human umbilical cord. STEM CELLS 2004;22:1330–1337.
6 Fu YS, Cheng YC, Lin MY et al. Conversion of human umbilical cord mesenchymal stem cells in Wharton's jelly to dopaminergic neurons in vitro: Potential therapeutic application for Parkinsonism. STEM CELLS 2006;24:115–124.
7 Weiss ML, Medicetty S, Bledsoe AR et al. Human umbilical cord matrix stem cells: Preliminary characterization and effect of transplantation in a rodent model of Parkinson's disease. STEM CELLS 2006;24:781–792.

8 Weiss ML, Mitchell KE, Hix JE et al. Transplantation of porcine umbilical cord matrix cells into the rat brain. Exp Neurol 2003;182:288–299.
9 Davies JE. Human umbilical cord perivascular cells (HUCPVCs): A high yield source of MSCs. 12th Annual Meeting of the International Society of Cellular Therapy; May 4–7, 2006; Berlin, Germany.
10 Shi S, Gronthos S. Perivascular niche of postnatal mesenchymal stem cells in human bone marrow and dental pulp. J Bone Miner Res 2003; 18:696–704.
11 Haleem-Smith H, Derfoul A, Okafor C et al. Optimization of high-efficiency transfection of adult human mesenchymal stem cells. Mol Biotechnol 2005;30:9–20.
12 Simmons PJ, Torok-Storb B. Identification of stromal cell precursors in human bone marrow by a novel monoclonal antibody, STRO-1. Blood 1991;78:55–62.
13 Duda DG, Cohen KS, di Tomaso E et al. Differential CD146 expression on circulating versus tissue endothelial cells in rectal cancer patients: Implications for circulating endothelial and progenitor cells as biomarkers for antiangiogenic therapy. J Clin Oncol 2006;24:1449–1453.
14 Blann AD, Woywodt A, Bertolini F et al. Circulating endothelial cells. Biomarker of vascular disease. Thromb Haemost 2005;93:228–235.
15 Wu H, Riha GM, Yang H et al. Differentiation and proliferation of endothelial progenitor cells from canine peripheral blood mononuclear cells. J Surg Res 2005;126:193–198.
16 Baksh D, Davies JE, Zandstra PW. Adult human bone marrow-derived mesenchymal progenitor cells are capable of adhesion-independent survival and expansion. Exp Hematol 2003;31:723–732.
17 Weinand C, Pomerantseva I, Neville CM et al. Hydrogel-beta-TCP scaffolds and stem cells for tissue engineering bone. Bone 2006;38:555–563.
18 Wang Y, Kim UJ, Blasioli DJ et al. In vitro cartilage tissue engineering with 3D porous aqueous-derived silk scaffolds and mesenchymal stem cells. Biomaterials 2005;26:7082–7094.
19 Mauck RL, Byers BA, Yuan X et al. Regulation of Cartilaginous ECM Gene Transcription by Chondrocytes and MSCs in 3D Culture in Response to Dynamic Loading. Biomech Model Mechanobiol 2007;6: 113–125.
20 Dannowski H, Bednarz J, Reszka R et al. Lipid-mediated gene transfer of acidic fibroblast growth factor into human corneal endothelial cells. Exp Eye Res 2005;80:93–101.
21 Aluigi M, Fogli M, Curti A et al. Nucleofection is an efficient nonviral transfection technique for human bone marrow-derived mesenchymal stem cells. STEM CELLS 2006;24:454–461.
22 Hamada H, Kobune M, Nakamura K et al. Mesenchymal stem cells (MSC) as therapeutic cytoreagents for gene therapy. Cancer Sci 2005; 96:149–156.
23 Yue B, Lu B, Dai KR et al. BMP2 gene therapy on the repair of bone defects of aged rats. Calcif Tissue Int 2005;77:395–403.
24 McMahon JM, Conroy S, Lyons M et al. Gene transfer into rat mesenchymal stem cells: A comparative study of viral and nonviral vectors. Stem Cells Dev 2006;15:87–96.
25 Boland GM, Perkins G, Hall DJ et al. Wnt 3a promotes proliferation and suppresses osteogenic differentiation of adult human mesenchymal stem cells. J Cell Biochem 2004;93:1210–1230.
26 De Boer J, Siddappa R, Gaspar C et al. Wnt signaling inhibits osteogenic differentiation of human mesenchymal stem cells. Bone 2004;34: 818–826.